Editors' Suggestion

Photonic Topological Insulating Phase Induced Solely by Gain and Loss

Kenta Takata[1] and Masaya Notomi[1,2]
[1]Nanophotonics Center and NTT Basic Research Laboratories, NTT Corporation, 3-1 Morinosato-Wakamiya, Atsugi 243-0198, Kanagawa, Japan
[2]Department of Physics, Tokyo Institute of Technology, H-55, Ookayama 2-12-1, Meguro 152-8550, Japan

(Received 25 October 2017; published 20 November 2018)

We reveal a one-dimensional topological insulating phase induced solely by gain and loss control in non-Hermitian optical lattices. The system comprises units of four uniformly coupled cavities, where the successive two have loss; the others experience gain, and they are balanced under two magnitudes. The gain and loss parts are effectively *dimerized*, and a bulk band gap, topological transition, midgap topological edge, and interface states in finite systems can all be achieved by controlled pumping. We also clarify non-Hermitian topological invariants and edge states in gapless conditions.

DOI: 10.1103/PhysRevLett.121.213902

Controlling optical properties with external signals is a major purpose of photonics research [1], and it is largely associated with tailoring the refractive index. Recent studies have revealed that the imaginary part of the refractive index, namely gain and loss, can do much more than just tune the optical intensity. The key concept, parity-time ($\mathcal{PT}$) symmetry [2,3], was introduced for obtaining real spectra of quantum systems with non-Hermitian components. Its analogy in optics [4,5] corresponds to complex refractive index profiles with symmetric real parts and antisymmetric imaginary parts, i.e., $n(\mathbf{r}) = n^*(-\mathbf{r})$. Such a system can show an exceptional point (EP) [6] where its eigendetuning sharply changes from real to imaginary values [7,8] (spontaneous $\mathcal{PT}$ symmetry breaking). There are many interesting phenomena related to $\mathcal{PT}$ symmetry, including power oscillation [4,9], double refraction [4,10], Bloch oscillation [11,12], mode locking [13], coherent absorption [14–16], fast light [10,17,18], and unidirectional reflectivity [19–21]. Furthermore, nonlinearity-induced isolation [22,23], single-mode lasing [24,25], and beam steering [26] were achieved under controlled pumping.

To widen the scope of non-Hermitian optics [27,28], there are growing attempts to incorporate topological features to photonic systems with gain and loss. While Hermitian photonic topological phases [29–31] are based on celebrated discoveries such as the quantum Hall effect [32,33] and topological insulators [34,35], non-Hermitian topological optics originates from the theoretical question as to whether or not stable topological quantum states exist in non-Hermitian systems [36–40]. For photonics based on classical electromagnetic waves, however, it has been clarified that there exist topological states even when their eigenvalues are not real [41]. Researchers applied Su-Schrieffer-Heeger (SSH) photonic lattices [42] with relevant loss and experimentally confirmed their topological interface states [43] and topological transition [44]. Moreover, a photonic topological bound state with global $\mathcal{PT}$ symmetry was observed [45]. Even the lasing of such topological modes has recently been shown to be feasible [46–49].

Then, another question may arise: Can we create a topological insulating phase solely from gain and loss control? In previous studies of non-Hermitian optics, the emergence of nontrivial topologies was attributed to Hermitian factors, namely the magneto-optic effect [49], and lattice and coupling profiles of host systems [37,50–53]. Even though such systems are armed with non-Hermiticity, they take over original Hermitian topological characters predetermined by fabrication. Moreover, gain and loss in conventional non-Hermitian systems [27,28,54] only close frequency band gaps. Thus, they were considered to destroy topological insulating phases. In contrast, our aim is to generate a topological band gap solely by adding static gain and loss to a topologically trivial structure. Then, achieved topological features, including a well-defined topological number, should originate purely from non-Hermitian factors. Here, the gain and loss are readily tunable by multichannel current injection or properly masked optical pumping in various laser systems [18,26,46–48]. We will hence have full manipulability over the topological properties in optical circuits, such as a topological transition, and the number and position of topological states, simply by changing the gain and loss.

Here, we show theoretically a one-dimensional photonic lattice with the gain- and loss-induced reconfigurable topological insulating phase. We consider unit cells of four uniformly coupled resonators, with loss introduced into two successive cavities and gain introduced into the other two. The system then forms a pair of dimers by effective decoupling between cavities with gain and loss. This can result in a bulk band gap, topological transition, and midgap edge states for a wide range of parameters.

Topological interface states can also be achieved at a controlled boundary between the nontrivial and trivial lattices. Our scheme is unique in non-Hermiticity-based *midgap* topological states protected by their isolation from bulk states. Nonetheless, we also clarify system topological features in non-Hermitian gapless conditions, which will be relevant with defect and edge states in gapless systems [37,55–59].

Theoretical model.—The system comprises periods of four single-mode cavities with uniform couplings κ [Fig. 1(a)]. We introduce an on-site imaginary potential profile $(ig_1, -ig_2, -ig_1, ig_2)$ to the cavities, where its positive and negative coefficients mean gain and loss, respectively. Here, we assume that κ, g_1, and g_2 are sufficiently small compared to the cavities' resonant frequency ω_0 and the cavity-mode Q factor is high, so that we can safely neglect the effect of the imaginary index profile and radiation loss on κ, as expected in semiconductor lasers [18,22,23,25,26,46–48,60]. Within the linear analysis, the coupled mode equation describing the system is equivalent to the Schrödinger equation, $i\partial_t|\Psi\rangle = \hat{\mathcal{H}}|\Psi\rangle$, where $|\Psi\rangle = (\{\Psi_n\})^T$ is the vector of the slowly varying complex cavity-mode amplitudes (n is the cavity index) and $\hat{\mathcal{H}}$ is a tight-binding lattice Hamiltonian. Considering the Bloch theorem and a dynamical factor $e^{-i\omega t}$, the analysis reduces to an eigenvalue problem for the four-component eigenvector $|\psi_B\rangle$ under the Bloch Hamiltonian $\hat{\mathcal{H}}(k)$,

$$\hat{\mathcal{H}}(k) = \begin{pmatrix} ig_1 & \kappa & 0 & \kappa e^{-ika} \\ \kappa & -ig_2 & \kappa & 0 \\ 0 & \kappa & -ig_1 & \kappa \\ \kappa e^{ika} & 0 & \kappa & ig_2 \end{pmatrix}, \quad (1)$$

where a is the spatial interval between the four-cavity units and k is the Bloch wave number. The eigenfrequency detuning $\omega(k)$ with reference to ω_0 is given by

$$\omega(k) = \pm\frac{1}{\sqrt{2}}\sqrt{A \pm \sqrt{A^2 - B^2 - 16\kappa^4 \sin^2\frac{ka}{2}}}, \quad (2)$$

where $A = 4\kappa^2 - g_1^2 - g_2^2$ and $B = 2g_1g_2$. We also find analytic forms of $|\psi_{B,s}\rangle$ (s is the eigenstate index), which are given in Supplemental Material [61]. In the following analysis, the gain and loss are measured with respect to the cavity coupling, i.e., $\kappa = 1$. We focus on the case where $g_1 > 0$ and $g_1 \geq |g_2|$ for studying the bulk properties, because the spatial and/or time reversal can map the system with this condition to that with the other parameter range. When $g_1 = g_2 = 0$, the system has a gapless fourfold cosinusoidal band structure with a degeneracy at $\omega(0) = 0$, because of the reduced first Brillouin zone [Fig. 1(b)].

The system band structure is classified into five patterns via the value of the inside of the double radical sign of Eq. (2) for $k = 0$ [Fig. 1(c)]. With $g_1, g_2 \geq 0$ for simplicity, the divided phase regions are (I) $B = 0$, (II) $A + B > 0$, $A - B \geq 0$, (III) $A + B > 0$, $A - B < 0$, (IV) $A + B \leq 0$, $A^2 - B^2 - 16\kappa^4 < 0$, and (V) $A^2 - B^2 - 16\kappa^4 \geq 0$. Here, the phase boundaries are symmetric to $g_1 = g_2$. The systems in phase II and III have complete frequency band gaps, while those in phase I, IV, and V are gapless. System band structures for phase IV and V are shown elsewhere (Fig. S1 in Supplemental Material [61]). Note that the diagram for $g_2 < 0$ is obtained by the mirror inversion of Fig. 1(c) with regard to $g_2 = 0$.

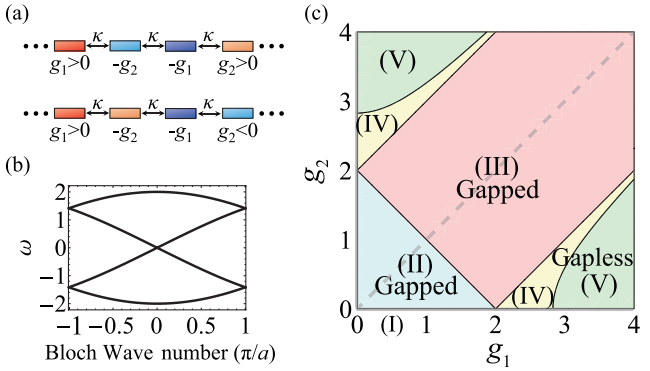

FIG. 1. (a) Schematic of considered system. Upper and lower lattices for $g_2 > 0$ and $g_2 < 0$ are topologically nontrivial and trivial, respectively. (b) Folded cosinusoidal band structure for $g_1 = g_2 = 0$. (c) Phase diagram for the system band structure. $\kappa = 1$, g_1, $g_2 \geq 0$.

We see from Eq. (2) that $\omega(k)$ is real as long as $A > 0$ and $A^2 - B^2 - 16\kappa^4 \sin^2(ka/2) > 0$. Such real eigenvalues are obtained because $\hat{\mathcal{H}}(k)$ has a pseudo-Hermiticity [70], $\hat{\mathcal{S}}(k)\hat{\mathcal{H}}(k)\hat{\mathcal{S}}(k) = \hat{\mathcal{H}}^\dagger(k)$. Here, the k-dependent linear operator $\hat{\mathcal{S}}(k) = \hat{\mathcal{S}}(k)^{-1} = \hat{\sigma}_x \otimes [\cos(k/2)]\hat{I}_2 + \hat{\sigma}_y \otimes [\sin(k/2)]\hat{I}_2$ means a half-period translation. $\hat{\sigma}_{x,y,z}$ are Pauli matrices and $\hat{I}_2$ is the 2×2 identity matrix. The pseudo-Hermiticity guarantees an associated antilinear symmetry [71]. Although the system does not respect $\mathcal{PT}$ symmetry, the bulk antilinear symmetry can instead give at least partially real spectra by balancing net gain and loss. Meanwhile, the operation to which $\hat{\mathcal{H}}(k)$ shows the invariance is implicit due to its complexity.

$\hat{\mathcal{H}}(k)$ also satisfies a pseudo-anti-Hermiticity [36,37,61], $\hat{\mathcal{H}}(k) = -\hat{\eta}\hat{\mathcal{H}}^\dagger(k)\hat{\eta}$, where $\hat{\eta} = \hat{I}_2 \otimes \hat{\sigma}_z = \mathrm{diag}(1, -1, 1, -1)$ and $\hat{\eta}^{-1} = \hat{\eta}^\dagger = \hat{\eta}$ in our model. It is known that this symmetry can lead to a nontrivial topology via *chirality* in terms of pairwise eigenvalues, $\omega(k)$ and $-\omega^*(k)$. Since $\hat{\eta}$ is local (diagonal), the resultant topological protection covers all the system parameters. We notice that the symmetry is equivalent to a particle-hole symmetry, $-\hat{\mathcal{H}}(k) = \hat{\eta}\hat{\mathcal{H}}^*(-k)\hat{\eta}$.

Bulk properties.—Figure 2 shows the real and imaginary band structures and eigenmode distributions for different g_1 and g_2 values. When $g_1 < 2$ and $g_2 = 0$ (phase I with

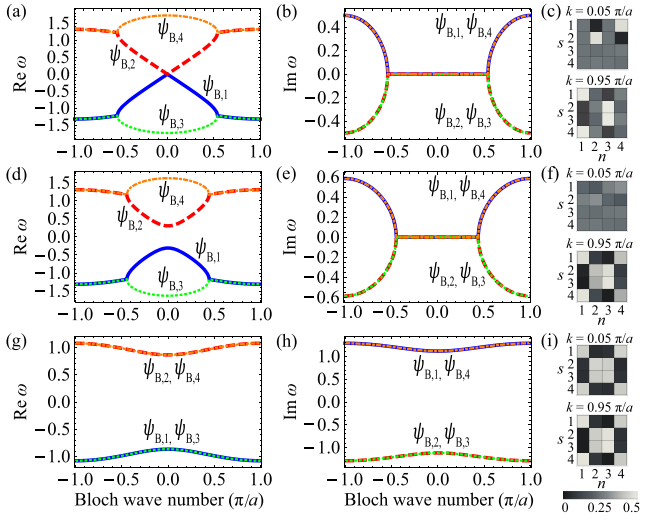

FIG. 2. Band structures and mode patterns of system for different gain and loss profiles. $\kappa = 1$. (a) Re$\omega(k)$, (b) Im$\omega(k)$, and (c) $|\psi_{B,s,n}|^2/\langle\psi_{B,s}|\psi_{B,s}\rangle$ for $g_1 = 1$, $g_2 = 0$, phase I. (d) Re$\omega(k)$, (e) Im$\omega(k)$, and (f) $|\psi_{B,s,n}|^2/\langle\psi_{B,s}|\psi_{B,s}\rangle$ for $g_1 = 1$, $g_2 = 0.5$, phase II. (g) Re$\omega(k)$, (h) Im$\omega(k)$, and (i) $|\psi_{B,s,n}|^2/\langle\psi_{B,s}|\psi_{B,s}\rangle$ for $g_1 = 2$, $g_2 = 1$, phase III. s and n are eigenstate and cavity indices, respectively.

$A > 0$), Dirac-like dispersion in Re$\omega(k)$ [Fig. 2(a)] appears around $\omega(0) = 0$, with canceled net gain and loss [Im$\omega(k) = 0$, Fig. 2(b)]. This implies a topological transition point and reflects the antilinear symmetry. The gapless feature is attributed to $B = 0$ in Eq. (2). The band structure also has two EPs that mean spontaneous antilinear symmetry breaking. The intensity distributions for $|\psi_{B,s}\rangle$ [Fig. 2(c)] show that the fields are evenly distributed in the gain and loss cavities ($n = 1$, 3) before this transition ($k = 0.05\pi/a$), while the eigenmodes with the broken symmetry ($k = 0.95\pi/a$) exhibit localization at either of them, and hence complex $\omega(k)$. Note that $g_1 > 2$ and $g_2 = 0$ (phase I, $A < 0$) give a Dirac cone in Im$\omega(k)$, with a degeneracy at $\omega(0) = 0$ (Fig. S1 in Supplemental Material [61]).

For g_1, $g_2 \neq 0$ under phase II, a band gap opens due to $B^2 > 0$ [$|g_2| \leq 2\kappa - g_1$, Fig. 2(c)], while the real eigenvalues remain around $k = 0$ [Fig. 2(d)]. Here, the effective couplings between gain and loss cavities become *weaker* than that between the two gain cavities and that between the loss cavities [61], as anticipated from the mode localization by $\mathcal{PT}$ symmetry breaking [7,8,27,28]. This decoupling results in dimerization of the successsive cavities with gain and those with loss [61].

Bulk mode patterns in the insulating conditions confirm this non-Hermitian effect. Before crossing the EPs in phase II, the eigenmodes spread over the entire unit cell to cancel the net gain and loss for real $\omega(k)$ [$k = 0.05\pi/a$, Fig. 2(f)]. After the symmetry breaking, however, they eventually turn into couples of states with localization at the gain cavities ($n = 1$, 4) and loss cavities ($n = 2$, 3) for complex $\omega(k)$ ($k = 0.95\pi/a$). In phase III ($|g_2| > 2\kappa - g_1$), the complete antilinear symmetry breaking makes the pairs of upper and lower real bands overlap and gives the split imaginary bands [Figs. 2(g) and 2(h)]. Thus, only the dimerized eigenstates are allowed all over the Brillouin zone [Fig. 2(i)]. Here, reversing the signs of g_1 and g_2 does not affect the band structure [Eq. (2)], while a topological transition between systems with $g_2 > 0$ and $g_2 < 0$ is expected at the gap closing with $\omega(0) = 0$. The non-Hermiticity-based band gap broadens continuously as (g_1, g_2) gets toward the inside of phase II and III from their boundaries (Fig. S2 in Supplemental Material [61]).

We introduce the normalized global Berry phase [72] in k space, $W = \sum_s (i/4\pi) \oint dk \langle\langle\psi_{B,s}|\partial_k|\psi_{B,s}\rangle$ ($s = 1, \ldots, 4$), as our topological number. W denotes the topological feature of the entire system [73]; thus it resolves the problem that the Zak phase [74] of each band is not discretized in non-Hermitian systems with EPs. Here, $|\psi_{B,s}\rangle\rangle$ is the left eigenstate that forms a duality with $|\psi_{B,s}\rangle$, namely, $\hat{\mathcal{H}}(k)|\psi_{B,s}\rangle = \omega(k)|\psi_{B,s}\rangle$ and $\hat{\mathcal{H}}^\dagger(k)|\psi_{B,s}\rangle\rangle = \omega^*(k)|\psi_{B,s}\rangle\rangle$ [75]. The biorthonormal basis $(\{|\psi_{B,s}\rangle\}, \{|\psi_{B,s}\rangle\rangle\})$ enables the normalization $\langle\langle\psi_{B,s}|\psi_{B,t}\rangle = \delta_{s,t}$ and the extraction of pure geometric phases from non-Hermitian eigenvectors. W also reflects the 4π periodicity of the eigenvectors [52,61]. We obtain integer values of $W = 1$ for $g_2 > 0$ and $W = 0$ for $g_2 < 0$, under $g_1 > 0$ (Fig. S3 of Supplemental Material [61]). W hence confirms the non-Hermiticity-induced nontrivial photonic topology and topological transition between the two conditions in Fig. 1(a). Interestingly, the discrete change in W holds in the gapless phases, IV and V. We discuss a geometric picture of W, which is based on coupling parameters relevant with dimerization and can illustrate the topological transition of both the SSH and our model, in Supplemental Material [61] (Figs. S4 and S5).

Edge states.—Figure 3 shows the topological edge states in our finite systems with 40 cavities for $g_1 > 0$, $g_2 > 0$. Here, there is relatively weaker effective coupling between gain and loss cavities at each edge [Fig. 3(a)], like the edge-state generation condition in the Hermitian SSH model [42,50]. Displayed eigenfrequencies show a pair of midgap states for both phase II [Fig. 3(b)] and phase III [Fig. 3(d)]. For Fig. 3(d), we consider an offset absorption potential $i\gamma$ for every cavity, which only shifts all the eigenfrequencies by $i\gamma$ and cancels Imω of a midgap state. Each eigenmode with Re$\omega = 0$ is localized at the left or right edge. Their Imω reflect the imaginary potential around the relevant edge cavities. A remarkable difference is whether the localization is unit based [phase II, Fig. 3(c)] or cavity based [phase III, Fig. 3(e)], corresponding to whether the bulk without the imaginary offset is in the *exact* phase [Im$\omega(0) = 0$] or *broken* phase [Im$\omega(0) \neq 0$]. In phase III, a topological edge mode has the largest Imω and can be the only state that oscillates (Im$\omega = 0$) via the loss offset, $\gamma < 0$ [Fig. 3(d)]. Note that the edge states are also found

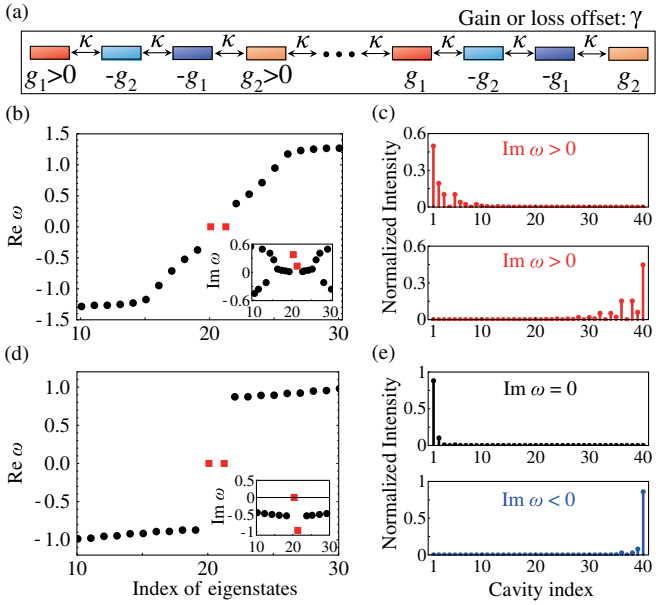

FIG. 3. (a) Illustration of our finite non-Hermitian topological lattice. (b),(d) Sorted and selected real eigenvalues for forty-cavity systems. Insets: Corresponding imaginary eigenvalues. Red squares are topological edge states. (c),(e) Intensity distributions for the edge states. (b),(c) $g_1 = 1$, $g_2 = 0.5$, $\gamma = 0$. (d),(e) $g_1 = 2$, $g_2 = 1$, $\gamma \sim -1.569$.

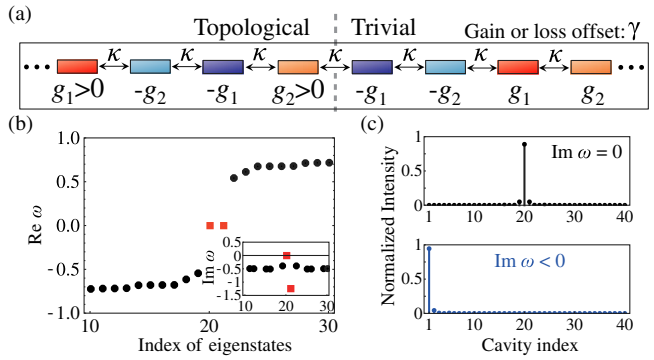

FIG. 4. (a) Interface between topologically nontrivial (left) and trivial (right) lattices, with 20 cavities for each. (b) Sorted and selected Reω of the system. Inset: Corresponding Imω. Left and right red squares are eigenvalues for topological interface and edge states. (c) Intensity profiles for the interface (upper) and edge (lower) modes. $g_1 = 1.5$, $g_2 = 3$, $\gamma \sim -2.526$.

when each side is terminated by a loss cavity ($g_1 < 0$, $g_2 < 0$). However, they disappear if a cavity on one edge has gain and one on the other undergoes loss ($g_1 g_2 < 0$), as indicated by $W = 0$. In Supplemental Material [61], we show detuned edge states for $g_1 = g_2$, striking robustness of the edge states to disorder, and edge states in the gapless phases (Figs. S6, S7, S8, and S9).

The topological vortex charge of non-Hermitian bulk eigendetuning [57], $V = (1/2\pi)\int \partial_k \mathrm{Arg}[\omega(k)]dk$, can be evaluated for our model [61]. Here, finite fractional charges $V = \pm 1/2$ are found around two degenerate EPs with $\omega = 0$ in the gapless phase IV [Fig. S10(a) of Supplemental Material [61]]. They indicate anomalous edge states with non-Hermitian chirality emerging at Re$\omega = 0$, and such states are compatible with both the topologically nontrivial ($W = 1$) and trivial ($W = 0$) systems. In phase V, $V = \pm 1/2$ is held by each eigenstate of the non-Hermitian flatband with Re$\omega = 0$ [Fig. S10(b) of Supplemental Material [61]].

We can discuss the origin of the topological edge states with a particle-hole symmetry [76] equivalent to our pseudo-anti-Hermiticity. Because our lattice Hamiltonian $\hat{\mathcal{H}}$ with a finite number of cavities and the open boundary condition is a symmetric matrix ($\hat{\mathcal{H}} = \hat{\mathcal{H}}^T$), its global pseudo-anti-Hermiticity, $\hat{\mathcal{H}} = -\hat{\eta}'\hat{\mathcal{H}}^\dagger\hat{\eta}'$, easily reduces to a particle-hole symmetry, $-\hat{\mathcal{H}} = \hat{\eta}'\hat{\mathcal{H}}^*\hat{\eta}'$. Here, $\hat{\eta}' = \mathrm{diag}(1, -1, 1, -1, \ldots, 1, -1, 1, -1)$ is again local, $\hat{\eta}'^{-1} = \hat{\eta}'^\dagger = \hat{\eta}'$, and $\hat{\mathcal{H}}^*$ is the complex conjugate of $\hat{\mathcal{H}}$. It indicates that the number of states with Re$\omega = 0$ at each edge can change only by two [77,78]. Thus, a single isolated edge state with Re$\omega = 0$ on each side, based on $(1, 0, 0, \ldots, 0)^T$ and $(0, \ldots, 0, 0, 1)^T$ for $g_1 = g_2 = 0$, is topologically protected by this symmetry under proper band gap-opening conditions [79].

Interface states.—We apply our non-Hermitian scheme for a controllable midgap topological interface state (Fig. 4). Here, we prepare butting of topologically nontrivial and trivial lattices, effectively forming a "long-long defect" at their boundary, as in a SSH system [80] [Fig. 4(a)]. Both lattices are adjusted to be in phase III, and larger gain is applied to the interface cavity of the nontrivial array than its edge ($g_2 > g_1$). In consequence, a topological interface state with Re$\omega = 0$ and strong boundary localization obtains the largest Imω as the abovementioned edge state. Including a global loss bias $i\gamma$, we can hence expect single-mode lasing (Im$\omega = 0$) of such a state. The system eigenfrequency profile [Fig. 4(b)] confirms a pair of midgap states and cancellation of Imω in one of them. The intensity distributions of the eigenmodes with $\omega = 0$ and Re$\omega = 0$, Im$\omega < 0$ certainly indicate topological interface and edge states confined at the right ($n = 20$) and left ($n = 1$) sides of the nontrivial lattice, respectively [Fig. 4(c)]. A topological bound state with global $\mathcal{PT}$ symmetry, which systematically satisfies Reω = Im$\omega = 0$, can also be demonstrated (Fig. S11 of Supplemental Material [61]).

In conclusion, we have shown that the topological insulating properties of the one-dimensional resonator array can be controlled by the gain and loss. Our scheme is experimentally feasible by modifying the existing laser arrays [46–48] and is valid for coupled waveguides [44,45]. Moreover, it can be explored as an extension of $\mathcal{PT}$-symmetric systems in photonics [10,18,22–26,43], phononics [81–83], and circuit electronics [84,85]. It would

pave the way for various possibilities of non-Hermitian topological photonics, such as reconfigurable lasing modes, non-Hermiticity-based topological pumping [41,86], superstructures [87], and Floquet systems [40,88]. Developing the topological controllability in two dimension is another important direction.

We thank Hiroshi Yamaguchi, Kensuke Inaba, and Koji Muraki for fruitful discussions. We acknowledge financial support from the Japan Science and Technology Agency (JST) through the CREST program under Grant No. JPMJCR15N4.

[1] A. Yariv and P. Yeh, *Photonics: Optical Electronics in Modern Communications*, 6th ed. (Oxford University Press, New York, 2007).
[2] C. M. Bender and S. Boettcher, Phys. Rev. Lett. **80**, 5243 (1998).
[3] C. M. Bender, D. C. Brody, and H. F. Jones, Phys. Rev. Lett. **89**, 270401 (2002).
[4] K. G. Makris, R. El-Ganainy, D. N. Christodoulides, and Z. H. Musslimani, Phys. Rev. Lett. **100**, 103904 (2008).
[5] Z. H. Musslimani, K. G. Makris, R. El-Ganainy, and D. N. Christodoulides, Phys. Rev. Lett. **100**, 030402 (2008).
[6] S. Klaiman, U. Günther, and N. Moiseyev, Phys. Rev. Lett. **101**, 080402 (2008).
[7] A. Guo, G. J. Salamo, D. Duchesne, R. Morandotti, M. Volatier-Ravat, V. Aimez, G. A. Siviloglou, and D. N. Christodoulides, Phys. Rev. Lett. **103**, 093902 (2009).
[8] C. E. Rüter, K. G. Makris, R. El-Ganainy, D. N. Christodoulides, M. Segev, and D. Kip, Nat. Phys. **6**, 192 (2010).
[9] I. V. Barashenkov, S. V. Suchkov, A. A. Sukhorukov, S. V. Dmitriev, and Y. S. Kivshar, Phys. Rev. A **86**, 053809 (2012).
[10] A. Regensburger, C. Bersch, M.-A. Miri, G. Onishchukov, D. N. Christodoulides, and U. Peschel, Nature (London) **488**, 167 (2012).
[11] S. Longhi, Phys. Rev. Lett. **103**, 123601 (2009).
[12] M. Wimmer, M.-A. Miri, D. Christodoulides, and U. Peschel, Sci. Rep. **5**, 17760 (2015).
[13] S. Longhi, Opt. Lett. **41**, 4518 (2016).
[14] Y. D. Chong, L. Ge, H. Cao, and A. D. Stone, Phys. Rev. Lett. **105**, 053901 (2010).
[15] S. Longhi, Phys. Rev. A **82**, 031801(R) (2010).
[16] Y. Sun, W. Tan, H.-Q. Li, J. Li, and H. Chen, Phys. Rev. Lett. **112**, 143903 (2014).
[17] A. Szameit, M. C. Rechtsman, O. Bahat-Treidel, and M. Segev, Phys. Rev. A **84**, 021806(R) (2011).
[18] K. Takata and M. Notomi, Phys. Rev. Applied **7**, 054023 (2017).
[19] Z. Lin, H. Ramezani, T. Eichelkraut, T. Kottos, H. Cao, and D. N. Christodoulides, Phys. Rev. Lett. **106**, 213901 (2011).
[20] L. Feng, Y.-L. Xu, W. S. Fegadolli, M.-H. Lu, J. E. B. Oliveira, V. R. Almeida, Y.-F. Chen, and A. Scherer, Nat. Mater. **12**, 108 (2013).
[21] H. Ramezani, H.-K. Li, Y. Wang, and X. Zhang, Phys. Rev. Lett. **113**, 263905 (2014).
[22] B. Peng, S. K. Özdemir, F. Lei, F. Monifi, M. Gianfreda, G. L. Long, S. Fan, F. Nori, C. M. Bender, and L. Yang, Nat. Phys. **10**, 394 (2014).
[23] L. Chang, X. Jiang, S. Hua, C. Yang, J. Wen, L. Jiang, G. Li, G. Wang, and M. Xiao, Nat. Photonics **8**, 524 (2014).
[24] L. Feng, Z. J. Wong, R.-M. Ma, Y. Wang, and X. Zhang, Science **346**, 972 (2014).
[25] H. Hodaei, M.-A. Miri, M. Heinrich, D. N. Christodoulides, and M. Khajavikhan, Science **346**, 975 (2014).
[26] Z. Gao, S. T. M. Fryslie, B. J. Thompson, P. S. Carney, and K. D. Choquette, Optica **4**, 323 (2017).
[27] L. Feng, R. El-Ganainy, and L. Ge, Nat. Photonics **11**, 752 (2017).
[28] R. El-Ganainy, K. G. Makris, M. Khajavikhan, Z. H. Musslimani, S. Rotter, and D. N. Christodoulides, Nat. Phys. **14**, 11 (2018).
[29] F. D. M. Haldane and S. Raghu, Phys. Rev. Lett. **100**, 013904 (2008).
[30] L. Lu, J. D. Joannopoulos, and M. Soljačić, Nat. Photonics **8**, 821 (2014).
[31] L. Lu, J. D. Joannopoulos, and M. Soljačić, Nat. Phys. **12**, 626 (2016).
[32] K. v. Klitzing, G. Dorda, and M. Pepper, Phys. Rev. Lett. **45**, 494 (1980).
[33] D. J. Thouless, M. Kohmoto, M. P. Nightingale, and M. den Nijs, Phys. Rev. Lett. **49**, 405 (1982).
[34] C. L. Kane and E. J. Mele, Phys. Rev. Lett. **95**, 146802 (2005).
[35] M. Z. Hasan and C. L. Kane, Rev. Mod. Phys. **82**, 3045 (2010).
[36] M. Sato, K. Hasebe, K. Esaki, and M. Kohmoto, Prog. Theor. Phys. **127**, 937 (2012).
[37] K. Esaki, M. Sato, K. Hasebe, and M. Kohmoto, Phys. Rev. B **84**, 205128 (2011).
[38] Y. C. Hu and T. L. Hughes, Phys. Rev. B **84**, 153101 (2011).
[39] C. Yuce, Phys. Lett. A **379**, 1213 (2015).
[40] C. Yuce, Eur. Phys. J. D **69**, 184 (2015).
[41] H. Schomerus, Opt. Lett. **38**, 1912 (2013).
[42] W. P. Su, J. R. Schrieffer, and A. J. Heeger, Phys. Rev. Lett. **42**, 1698 (1979).
[43] C. Poli, M. Bellec, U. Kuhl, F. Mortessagne, and H. Schomerus, Nat. Commun. **6**, 6710 (2015).
[44] J. M. Zeuner, M. C. Rechtsman, Y. Plotnik, Y. Lumer, S. Nolte, M. S. Rudner, M. Segev, and A. Szameit, Phys. Rev. Lett. **115**, 040402 (2015).
[45] S. Weimann, M. Kremer, Y. Plotnik, Y. Lumer, S. Nolte, K. G. Makris, M. Segev, M. C. Rechtsman, and A. Szameit, Nat. Mater. **16**, 433 (2017).
[46] P. St-Jean, V. Goblot, E. Galopin, A. Lemaître, T. Ozawa, L. L. Gratiet, I. Sagnes, J. Bloch, and A. Amo, Nat. Photonics **11**, 651 (2017).
[47] M. Parto, S. Wittek, H. Hodaei, G. Harari, M. A. Bandres, J. Ren, M. C. Rechtsman, M. Segev, D. N. Christodoulides, and M. Khajavikhan, Phys. Rev. Lett. **120**, 113901 (2018).
[48] H. Zhao, P. Miao, M. H. Teimourpour, S. Malzard, R. El-Ganainy, H. Schomerus, and L. Feng, Nat. Commun. **9**, 981 (2018).
[49] B. Bahari, A. Ndao, F. Vallini, A. E. Amili, Y. Fainman, and B. Kanté, Science **358**, 636 (2017).

[50] N. Malkova, I. Hromada, X. Wang, G. Bryant, and Z. Chen, Opt. Lett. **34**, 1633 (2009).
[51] S. Aubry and G. André, Ann. Isr. Phys. Soc. **3**, 133 (1980).
[52] T. E. Lee, Phys. Rev. Lett. **116**, 133903 (2016).
[53] G. Q. Liang and Y. D. Chong, Phys. Rev. Lett. **110**, 203904 (2013).
[54] H. Kogelnik and C. V. Shank, J. Appl. Phys. **43**, 2327 (1972).
[55] S. Malzard, C. Poli, and H. Schomerus, Phys. Rev. Lett. **115**, 200402 (2015).
[56] H. Zhao, S. Longhi, and L. Feng, Sci. Rep. **5**, 17022 (2015).
[57] D. Leykam, K. Y. Bliokh, C. Huang, Y. D. Chong, and F. Nori, Phys. Rev. Lett. **118**, 040401 (2017).
[58] B. Qi, L. Zhang, and L. Ge, Phys. Rev. Lett. **120**, 093901 (2018).
[59] M. Pan, H. Zhao, P. Miao, S. Longhi, and L. Feng, Nat. Commun. **9**, 1308 (2018).
[60] J. K. S. Poon and A. Yariv, J. Opt. Soc. Am. B **24**, 2378 (2007).
[61] See Supplemental Material at http://link.aps.org/supplemental/10.1103/PhysRevLett.121.213902 for the system gapless phases, bulk symmetry, effective decoupling, band gap opening, topological number and its geometrical picture, possible finite size effects, robustness of the topological edge states, chiral edge states in gapless phases, vortex charges of eigendetuning with band coalescence, and non-Hermiticity-based topological bound state with $\mathcal{PT}$ symmetry, which includes Refs. [62–69].
[62] B. Zhen, C. W. Hsu, Y. Igarashi, L. Lu, I. Kaminer, A. Pick, S.-L. Chua, J. D. Joannopoulos, and M. Soljačić, Nature (London) **525**, 354 (2015).
[63] M. Berry, Czech. J. Phys. **54**, 1039 (2004).
[64] W. D. Heiss, J. Phys. A **45**, 444016 (2012).
[65] F. H. M. Faisal and J. V. Moloney, J. Phys. B **14**, 3603 (1981).
[66] T. E. Lee, Reply to comment on "Anomalous edge state in a non-Hermitian lattice," arXiv:1611.00355.
[67] P. Delplace, D. Ullmo, and G. Montambaux, Phys. Rev. B **84**, 195452 (2011).
[68] C. Yin, H. Jiang, L. Li, R. Lü, and S. Chen, Phys. Rev. A **97**, 052115 (2018).
[69] X.-F. Zhu, Opt. Express **23**, 22274 (2015).
[70] A. Mostafazadeh, J. Math. Phys. (N.Y.) **43**, 205 (2002).
[71] A. Mostafazadeh, J. Math. Phys. (N.Y.) **43**, 3944 (2002).
[72] S.-D. Liang and G.-Y. Huang, Phys. Rev. A **87**, 012118 (2013).
[73] Y. Hatsugai, J. Phys. Soc. Jpn. **73**, 2604 (2004).
[74] J. Zak, Phys. Rev. Lett. **62**, 2747 (1989).
[75] F. Keck, H. J. Korsch, and S. Mossmann, J. Phys. A **36**, 2125 (2003).
[76] S. Ryu, A. P. Schnyder, A. Furusaki, and A. W. W. Ludwig, New J. Phys. **12**, 065010 (2010).
[77] D. I. Pikulin and Y. V. Nazarov, JETP Lett. **94**, 693 (2012).
[78] D. I. Pikulin and Y. V. Nazarov, Phys. Rev. B **87**, 235421 (2013).
[79] S. Ryu and Y. Hatsugai, Phys. Rev. Lett. **89**, 077002 (2002).
[80] A. Blanco-Redondo, I. Andonegui, M. J. Collins, G. Harari, Y. Lumer, M. C. Rechtsman, B. J. Eggleton, and M. Segev, Phys. Rev. Lett. **116**, 163901 (2016).
[81] H. Jing, S. K. Özdemir, X.-Y. Lü, J. Zhang, L. Yang, and F. Nori, Phys. Rev. Lett. **113**, 053604 (2014).
[82] X. Zhu, H. Ramezani, C. Shi, J. Zhu, and X. Zhang, Phys. Rev. X **4**, 031042 (2014).
[83] X.-Y. Lü, H. Jing, J.-Y. Ma, and Y. Wu, Phys. Rev. Lett. **114**, 253601 (2015).
[84] J. Schindler, A. Li, M. C. Zheng, F. M. Ellis, and T. Kottos, Phys. Rev. A **84**, 040101 (2011).
[85] B. Lv, J. Fu, B. Wu, R. Li, Q. Zeng, X. Yin, Q. Wu, L. Gao, W. Chen, Z. Wang, Z. Liang, A. Li, and R. Ma, Sci. Rep. **7**, 40575 (2017).
[86] Y. E. Kraus, Y. Lahini, Z. Ringel, M. Verbin, and O. Zilberberg, Phys. Rev. Lett. **109**, 106402 (2012).
[87] A. A. Burkov and L. Balents, Phys. Rev. Lett. **107**, 127205 (2011).
[88] M. C. Rechtsman, J. M. Zeuner, Y. Plotnik, Y. Lumer, D. Podolsky, F. Dreisow, S. Nolte, M. Segev, and A. Szameit, Nature (London) **496**, 196 (2013).